Computer Assisted Mechanics and Engineering Sciences, 5: 31–44, 1998.

Numerical results on the locking for cylindrical shells

Claudia Chinosi, Lucia Della Croce and Terenzio Scapolla
Dipartimento di Matematica, Università di Pavia, I-27100 Pavia, Italy

(Received September 30, 1996)

We investigate the performance of the Naghdi shell model using a family of hierarchic high order finite elements. We solve two cylindrical shell problems, representative of extremely discriminating situations: the membrane dominated Scordelis–Lo problem and a bending dominated problem already tested by Leino and Pitkäranta. As it is well known, these problems are hard tests for shell elements, especially when the thickness of the shell is approaching to zero, since the presence of hidden constraints can lead to numerical convergence problems, known as shear and membrane locking. The numerical results show the robustness of the finite elements developed, able to avoid the locking behavior.

1. Introduction

In this paper we have considered the shell model arising from the Naghdi formulation. A displacement finite element scheme has been developed using C^0 finite element of hierarchic type of degree ranging from 1 to 4. In order to analyze the behavior of our finite elements respect to the membrane and shear locking, we have dealt with two test problems often used to assess the performance of numerical formulations based on the degenerated solid approach. The two tests are representative of extremely discriminating situations.

The first one is the well known Scordelis–Lo problem. It is a membrane dominated problem and it is used to evaluate the ability of the shell elements to capture complex membrane state of stress. We have evaluated the values of the displacement for different values of the thickness of the shell. The numerical results, especially for the elements of degree 3 and 4, show a good agreement with all the available benchmark results.

The second test refers to a partially clamped hemicylindrical shell. It is a bending dominated problem and it is a severe test for a shell element performance with respect to both membrane and shear locking (see [2, 4]). Our numerical experiences indicate that high order elements perform very well in both the test problems.

The outline of the paper is the following. In Section 2 first we describe the Naghdi's model for cylindrical shells; then we recall the mathematical model and introduce the finite elements used for the numerical approximation. In Section 3 we present an extensive set of numerical results. We consider a bending–dominated problem and a membrane–dominated problem. For each of the two tests we analyze in details the behavior of the finite element results versus the thickness of the shell structure.

2. Naghdi's model for cylindrical shells

2.1. The geometrical problem

Let us consider some model problems where the shape of the shell is cylindrical. In a system of Cartesian coordinates (O, x_1, x_2, x_3) the region occupied by the shell is in this case

$$S = \left\{ (x_1, x_2, x_3) \in \mathbb{R}^3 : \; -\frac{L}{2} < x_1 < \frac{L}{2}, \; \left(R - \frac{t}{2}\right)^2 < x_2^2 + x_3^2 < \left(R + \frac{t}{2}\right)^2 \right\} \tag{1}$$

where L, R and t denote the length, the radius and the thickness of the shell respectively.

Let us take a curvilinear coordinate system (ξ_1, ξ_2) placed at the centre of the midsurface, with

$$\begin{aligned} \xi_1 &= x_1 \\ \xi_2 &= R\theta \qquad \theta \in [-\pi, \pi]. \end{aligned} \tag{2}$$

The midsurface S of the shell is described by the mapping:

$$\vec{\varphi}(\xi_1, \xi_2) : \; \bar{\Omega} \subset \mathbb{R}^2 \longrightarrow \bar{S} \subset \mathbb{R}^3, \tag{3}$$

$$\begin{cases} \varphi_1(\xi_1, \xi_2) = \xi_1, \\ \varphi_2(\xi_1, \xi_2) = R \sin \dfrac{\xi_2}{R}, \\ \varphi_3(\xi_1, \xi_2) = R \cos \dfrac{\xi_2}{R}. \end{cases} \tag{4}$$

With such choices the region $\Omega \subset \mathbb{R}^2$ corresponding to the midsurface S is the rectangle

$$\Omega = \left\{ (\xi_1, \xi_2) : -\frac{L}{2} < \xi_1 < \frac{L}{2}, \; -R\pi < \xi_2 < R\pi \right\} \tag{5}$$

and the *covariant basis* at the point $\vec{\varphi}(\xi_1, \xi_2)$ of the midsurface S is

$$\begin{aligned} \vec{a}_1 &= (1, \, 0, \, 0), \\ \vec{a}_2 &= \left(0, \, \cos \frac{\xi_2}{R}, \, -\sin \frac{\xi_2}{R}\right), \\ \vec{a}_3 &= \left(0, \, \sin \frac{\xi_2}{R}, \, \cos \frac{\xi_2}{R}\right). \end{aligned} \tag{6}$$

It is known that $\vec{a}_3$ is normal to the undeformed middle surface. For each point $(\xi_1, \xi_2) \in \bar{\Omega}$ we consider a third coordinate ξ_3 along the direction $\vec{a}_3$ normal to the surface $\bar{S}$ at the point $\vec{\varphi}(\xi_1, \xi_2)$. The set (ξ_1, ξ_2, ξ_3) defines locally a system of curvilinear coordinates.

2.2. The mathematical model

The Naghdi model describes the deformation of a shell subject to a transverse loading when transverse shear deformation is taken into account. In Naghdi's approach constant shear deformation are allowed across the thickness of the shell. The main assumption is that particles lying on the direction $\vec{a}_3$ remain on a straight line during deformation, but the line does not necessarily keep normal to the deformed middle surface. With such an assumption the normal unit vector $\vec{a}_3$ is allowed a rotation $\vec{\theta}$ with covariant components θ_1, θ_2, i.e., $\vec{\theta} = \theta_\alpha \vec{a}_\alpha$.

The displacement $\vec{U}$ of a point belonging to the three–dimensional shell has the form:

$$\vec{U} = u_i \vec{a}_i + \xi_3 \theta_\alpha \vec{a}_\alpha \tag{7}$$

where u_i are the covariant components of the displacement $\vec{u} = (u_1, u_2, u_3)$ of the point $\vec{\varphi}(\xi_1, \xi_2)$ of the middle surface S.

Let us suppose that the shell is homogeneous and isotropic. As usual we denote by E, ν and k the Young's modulus, the Poisson ratio and the shear correction factor respectively. Hereafter the

value $k = 1$ is taken. The external forces acting on the shell can be written in terms of its covariant components p_i, i.e.,

$$\vec{p} = p_i \vec{a}_i \,. \tag{8}$$

For an arbitrary displacement field $\vec{u} = (u_i)$ and rotation field $\widetilde{\theta} = (\theta_\alpha)$, with u_i, θ_α in $H^1(\Omega)$, we define the change of curvature tensor Υ, the transverse shear strain tensor Σ, the membrane strain tensor Λ:

$$\begin{aligned}
\Upsilon_{11}(\vec{u},\widetilde{\theta}) &= \theta_{1,1}\,,\\
\Upsilon_{12}(\vec{u},\widetilde{\theta}) &= \frac{1}{2}\left(\theta_{1,2}+\theta_{2,1}+\frac{1}{R}u_{2,1}\right),\\
\Upsilon_{22}(\vec{u},\widetilde{\theta}) &= \theta_{2,2}+\frac{1}{R}\left(u_{2,2}+\frac{1}{R}u_3\right),\\
\Sigma_1(\vec{u},\widetilde{\theta}) &= u_{3,1}+\theta_1\,,\\
\Sigma_2(\vec{u},\widetilde{\theta}) &= u_{3,2}-\frac{1}{R}u_2+\theta_2\,,\\
\Lambda_{11}(\vec{u}) &= u_{1,1}\,,\\
\Lambda_{12}(\vec{u}) &= \frac{1}{2}(u_{1,2}+u_{2,1})\,,\\
\Lambda_{22}(\vec{u}) &= u_{2,2}+\frac{1}{R}u_3\,.
\end{aligned} \tag{9}$$

The strain energy $\bar{E}$ of the shell can be written as the sum of three contributes: bending, shear and membrane energy. The energy functional has the following form

$$\begin{aligned}
\bar{E}(\vec{v},\widetilde{\psi}) &= E^B(\vec{v},\widetilde{\psi})+E^S(\vec{v},\widetilde{\psi})+E^M(\vec{v},\widetilde{\psi})\,,\\
E^B(\vec{v},\widetilde{\psi}) &= \frac{t^3}{2}b(\vec{v},\widetilde{\psi};\vec{v},\widetilde{\psi})\,,\\
E^S(\vec{v},\widetilde{\psi}) &= \frac{t}{2}s(\vec{v},\widetilde{\psi};\vec{v},\widetilde{\psi})\,,\\
E^M(\vec{v},\widetilde{\psi}) &= \frac{t}{2}m(\vec{v},\vec{v})\,.
\end{aligned} \tag{10}$$

The bilinear form associated to the bending component of the energy is defined as

$$\begin{aligned}
b(\vec{u},\widetilde{\theta};\vec{v},\widetilde{\psi}) = \frac{E}{24(1+\nu)}\int_\Omega \Big(&\frac{2}{1-\nu}\,\Upsilon_{11}(\vec{u},\widetilde{\theta})\,\Upsilon_{11}(\vec{v},\widetilde{\psi})+\frac{2\nu}{1-\nu}\,\Upsilon_{22}(\vec{u},\widetilde{\theta})\,\Upsilon_{11}(\vec{v},\widetilde{\psi})\\
&+4\,\Upsilon_{12}(\vec{u},\widetilde{\theta})\,\Upsilon_{12}(\vec{v},\widetilde{\psi})+\frac{2\nu}{1-\nu}\,\Upsilon_{11}(\vec{u},\widetilde{\theta})\,\Upsilon_{22}(\vec{v},\widetilde{\psi})\\
&+\frac{2}{1-\nu}\,\Upsilon_{22}(\vec{u},\widetilde{\theta})\,\Upsilon_{22}(\vec{v},\widetilde{\psi})\Big)\,\mathrm{d}\xi_1\mathrm{d}\xi_2\,.
\end{aligned} \tag{11}$$

The bilinear form associated to the shear component of the energy is the following

$$s(\vec{u},\widetilde{\theta};\vec{v},\widetilde{\psi}) = \frac{Ek}{2(1+\nu)}\int_\Omega \Big(\Sigma_1(\vec{u},\widetilde{\theta})\,\Sigma_1(\vec{v},\widetilde{\psi})+\Sigma_2(\vec{u},\widetilde{\theta})\,\Sigma_2(\vec{v},\widetilde{\psi})\Big)\,\mathrm{d}\xi_1\mathrm{d}\xi_2 \tag{12}$$

and the bilinear form associated to the membrane component of the energy is

$$\begin{aligned}
m(\vec{u},\vec{v}) = \frac{Ek}{2(1+\nu)}\int_\Omega \Big(&\frac{2}{1-\nu}\,\Lambda_{11}(\vec{u})\,\Lambda_{11}(\vec{v})+\frac{2\nu}{1-\nu}\,\Lambda_{22}(\vec{u})\,\Lambda_{11}(\vec{v})\\
&+4\,\Lambda_{12}(\vec{u})\,\Lambda_{12}(\vec{v})+\frac{2\nu}{1-\nu}\,\Lambda_{11}(\vec{u})\,\Lambda_{22}(\vec{v})\\
&+\frac{2}{1-\nu}\,\Lambda_{22}(\vec{u})\,\Lambda_{22}(\vec{v})\Big)\,\mathrm{d}\xi_1\mathrm{d}\xi_2\,.
\end{aligned} \tag{13}$$

The load energy has the form

$$E^L(\vec{v},\tilde{\psi}) = \int_\Omega \vec{p}\,\vec{v}\,\sqrt{a}\,\mathrm{d}\xi_1\mathrm{d}\xi_2\,. \tag{14}$$

Setting $\vec{f} = \frac{1}{t^3}\vec{p}$ and scaling likewise the strain energy $\bar{E}$, the total energy functional can be written as:

$$E(\vec{v},\tilde{\psi}) = \frac{1}{t^3}\bar{E}(\vec{v},\tilde{\psi}) - \int_\Omega \vec{f}\vec{v}\sqrt{a}\,\mathrm{d}\xi_1\mathrm{d}\xi_2\,. \tag{15}$$

According to the energy principle, the shell assumes a state of deformation such that the total energy E is minimized. We suppose that the shell is *clamped* on the subset of the boundary $\partial S_0 = \vec{\varphi}(\Gamma_0)\times[-\frac{t}{2},\frac{t}{2}]$ where $\Gamma_0 = \partial\Omega_0$ is a non empty subset of $\partial\Omega$.

We define the spaces:

$$\begin{aligned} V &= \{v \in H^1(\Omega) : v|_{\Gamma_0} = 0\}\,. \\ V^5 &= \{(\vec{v},\tilde{\psi}) : v_i, \psi_\alpha \in V\}\,. \end{aligned} \tag{16}$$

The solution of the Naghdi model is the pair $(\vec{u},\tilde{\theta})$ such that

$$(\vec{u},\tilde{\theta}) = \min_{(\vec{v},\tilde{\psi})\in V^5} E(\vec{v},\tilde{\psi})\,. \tag{17}$$

The corresponding variational formulation of the problem assumes the form

$$\begin{cases} \text{Find } (\vec{u},\tilde{\theta}) \in V^5 \text{ such that :} \\ \quad b(\vec{u},\tilde{\theta};\vec{v},\tilde{\psi}) + \dfrac{1}{t^2}s(\vec{u},\tilde{\theta};\vec{v},\tilde{\psi}) + \dfrac{1}{t^2}m(\vec{u},\vec{v}) = \displaystyle\int_\Omega \vec{f}\vec{v}\,\mathrm{d}\xi_1\mathrm{d}\xi_2 \qquad \forall(\vec{v},\tilde{\psi}) \in V^5. \end{cases} \tag{18}$$

2.3. The finite elements and the stiffness matrix

Let $\bar{\Omega}$ be a polygonal domain. Let us introduce a decomposition $\mathcal{T}_h$ of $\bar{\Omega}$ into quadrilateral elements $\mathcal{Q}_h$ such that $\bigcup_{\mathcal{Q}_h\in\mathcal{T}_h}\mathcal{Q}_h = \bar{\Omega}$. We consider the space

$$V_h = \left\{(\vec{v}_h,\tilde{\psi}_h) :\ (v_h)_i, (\psi_h)_\alpha \in W_p(\mathcal{T}_h)\right\} \tag{19}$$

where

$$W_p(\mathcal{T}_h) = \left\{w \in H^1(\Omega) :\ w|_{\mathcal{Q}_h} \in S_p(\mathcal{Q}_h) \quad \forall\mathcal{Q}_h \in \mathcal{T}_h\right\}, \qquad p = 1,2,3,4. \tag{20}$$

and $S_p(\mathcal{Q}_h)$ is a space of Serendipity type functions of degree p on each $\mathcal{Q}_h \in \mathcal{T}_h$.

The space $S_p(\mathcal{Q}_h)$ is constructed as follows. Let $\mathcal{P}_p$ be the spaces of polynomials defined on the square $[-1,1]\times[-1,1]$ of degree less or equal p in the two variables. We take all monomials of the space $\mathcal{P}_p$ and we add the following monomial terms:

1. the monomial $\{xy\}$ in the case $p = 1$;

2. the monomials $\{x^p y, xy^p\}$ in the case $p \geq 2$.

Let us give a matrix form of the approximation of the problem (18). We consider a basis for the space $W_p(\mathcal{T}_h)$ and let denote by $\vec{F}$ the corresponding vector of shape functions, i.e., $\vec{F} = (F_1, F_2, \ldots, F_N)$, where N is the dimension of the approximation space $W_p(\mathcal{T}_h)$. The expression of the elementary stiffness matrix for an element $\mathcal{Q}_h \in \mathcal{T}_h$ is given in Fig. 1, where the following notations have been

$$
\mathcal{K}_e = \begin{bmatrix}
C_b\left[\mathbf{B}_{xx} + \frac{1-\nu}{2}\mathbf{B}_{yy}\right] + C_s\mathbf{B} & C_b\left[\nu\mathbf{B}_{xy} + \frac{1-\nu}{2}\mathbf{B}_{yx}\right] & 0 & C_b\left[\frac{\nu}{R}\mathbf{B}_{xy} + \frac{1-\nu}{2R}\mathbf{B}_{yx}\right] & \frac{\nu}{R^2}C_b\mathbf{B}_x + C_s\mathbf{B}_x^T \\
 & C_b\left[\frac{1-\nu}{2}\mathbf{B}_{xx} + \mathbf{B}_{yy}\right] + C_s\mathbf{B} & 0 & C_b\left[\frac{1-\nu}{2R}\mathbf{B}_{xx} + \frac{1}{R}\mathbf{B}_{yy}\right] - \frac{1}{R}C_s\mathbf{B} & \frac{1}{R^2}C_b\mathbf{B}_y^T + C_s\mathbf{B}_y \\
 & & C_m\left[\mathbf{B}_{xx} + \frac{1-\nu}{2}\mathbf{B}_{yy}\right] & C_m\left[\nu\mathbf{B}_{xy} + \frac{1-\nu}{2}\mathbf{B}_{yx}\right] & \frac{\nu}{R}C_m\mathbf{B}_x \\
 & & & C_b\left[\frac{1-\nu}{2R^2}\mathbf{B}_{xx} + \frac{1}{R^2}\mathbf{B}_{yy}\right] + C_m\left[\frac{1-\nu}{2}\mathbf{B}_{xx} + \mathbf{B}_{yy}\right] + \frac{1}{R^2}C_s\mathbf{B} & \frac{1}{R^3}C_b\mathbf{B}_y - \frac{1}{R}C_s\mathbf{B}_y^T + \frac{1}{R}C_m\mathbf{B}_y \\
\text{symmetric} & & & & \frac{1}{R^4}C_b\mathbf{B} + \frac{1}{R^2}C_m\mathbf{B} + C_s\left[\mathbf{B}_{xx} + \mathbf{B}_{yy}\right]
\end{bmatrix}
$$

Fig. 1. The stiffness matrix $\mathcal{K}_e$

used:

$$\begin{aligned}
\mathbf{B} &= \int_{\mathcal{Q}_h} \vec{F}^T \vec{F}\, \mathrm{d}x\mathrm{d}y\,, \\
\mathbf{B}_x &= \int_{\mathcal{Q}_h} \vec{F}^T \vec{F}_{/x}\, \mathrm{d}x\mathrm{d}y\,, \qquad \mathbf{B}_y = \int_{\mathcal{Q}_h} \vec{F}^T \vec{F}_{/y}\, \mathrm{d}x\mathrm{d}y\,, \\
\mathbf{B}_{xx} &= \int_{\mathcal{Q}_h} \vec{F}^T_{/x} \vec{F}_{/x}\, \mathrm{d}x\mathrm{d}y\,, \qquad \mathbf{B}_{yy} = \int_{\mathcal{Q}_h} \vec{F}^T_{/y} \vec{F}_{/y}\, \mathrm{d}x\mathrm{d}y\,, \\
\mathbf{B}_{xy} &= \int_{\mathcal{Q}_h} \vec{F}^T_{/x} \vec{F}_{/y}\, \mathrm{d}x\mathrm{d}y\,, \qquad \mathbf{B}_{yx} = \int_{\mathcal{Q}_h} \vec{F}^T_{/y} \vec{F}_{/x}\, \mathrm{d}x\mathrm{d}y\,,
\end{aligned} \tag{21}$$

and

$$C_b = \frac{E}{12(1-\nu^2)}\,, \qquad C_s = \frac{Ekt^{-2}}{2(1+\nu)}\,, \qquad C_m = \frac{Ekt^{-2}}{1-\nu^2}\,. \tag{22}$$

The previous integrals are computed exactly using Gaussian classical quadrature formulas of order $(p+1) \times (p+1)$.

3. Numerical results

3.1. The bending-dominated problem and the membrane-dominated problem

Referring to the expression of the energy of a shell problem (see (10)) we recall the usual classification of such a problem (see [2, 4]). The deformation field $(\vec{u}, \tilde{\theta})$ is named *inextensional* if and only if it satisfies both the shear constraints and the membrane constraints, i.e., if

$$E^S(\vec{v}, \tilde{\psi}) + E^M(\vec{v}, \tilde{\psi}) = 0. \tag{23}$$

The problem is called *bending dominated* if the bending part of the energy dominates the total energy, i.e.

$$E^B(\vec{v}, \tilde{\psi}) \gg E^S(\vec{v}, \tilde{\psi}) + E^M(\vec{v}, \tilde{\psi}). \tag{24}$$

In bending dominated shell problems the deformation field is inextensional. As it is shown elsewhere (see [6]) the *membrane locking* phenomenon is related to an inadequate representation of inextensional deformation. Thus the numerical approximation of this class of problems is prone to the *membrane locking.*

The problem is called *membrane dominated* if the membrane part of the energy dominates the total energy, i.e.

$$E^B(\vec{v}, \tilde{\psi}) \ll E^S(\vec{v}, \tilde{\psi}) + E^M(\vec{v}, \tilde{\psi}). \tag{25}$$

This case is more natural and it is more frequently found in real cases. Since a substantial part of the strain energy is membrane energy, the representation of inextensional modes is not crucial in this problem and the membrane locking does not affect severely the results. Indeed, some elements with strong membrane locking will converge at a moderate rate in this type of problems. Nevertheless when the transverse shear strain effect is taken into account in the finite element model, the so called *shear locking* phenomenon occurs. We note that the discrimination between the bending and membrane dominated problem depends in general: (i) on the shell geometry; (ii) on the boundary conditions; (iii) on the load.

3.2. A membrane-dominated problem

We consider the Scordelis–Lo problem [1, 3, 5]. It deals with a cylindrical shell known in the literature as *barrel vault*. The shell is described in Fig. 2. We have the following data.

(i) Shell geometry. The region corresponding to the midsurface S is the rectangle

$$\Omega = \left\{(\xi_1, \xi_2) : -\frac{L}{2} < \xi_1 < \frac{L}{2},\ -R\frac{2\pi}{9} < \xi_2 < R\frac{2\pi}{9}\right\}. \tag{26}$$

(ii) Boundary conditions. The shell is simple supported on rigid diaphgrams and free on the other sides.

(iii) Load. The shell is loaded by its own weight.

The test is know as a membrane dominated problem [6] because a relation likewise (25) holds. Table 1 shows the physical data assumed in the test.

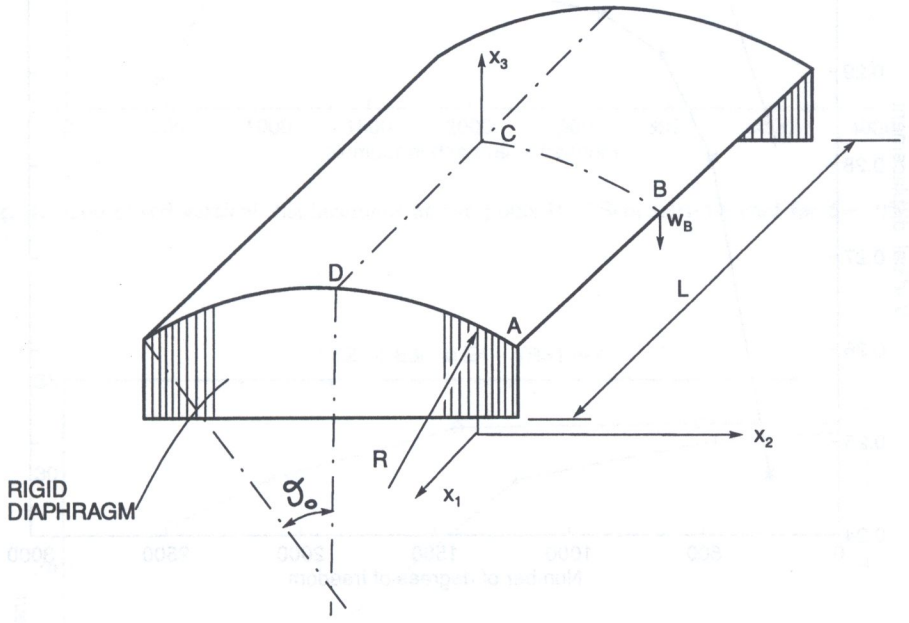

Fig. 2. Scordelis–Lo roof

Table 1. Physical data

quantity	name	value
Young's modulus	E	4.32×10^8 lb/ft^2
Poisson's ratio	ν	0.0
radius	R	25 ft
thickness	t/R	$10^{-2} \div 10^{-4}$
length	L	50 ft
angle	θ_0	$\frac{2\pi}{9}$ rad
specific weight	$s.w.$	.20626

The barrel vault has a symmetric structure; thus the computations have been performed only on a quarter of the shell using a uniform decomposition. The following symmetry conditions have been assumed:

$$u_2(\xi_1, 0) = \theta_2(\xi_1, 0) = 0,$$
$$u_1(0, \xi_2) = \theta_1(0, \xi_2) = 0. \tag{27}$$

In order to analyse the shear and the membrane locking arising in this test problem we have considered different values of the ratio t/R, although an interesting case is the one with the value of $t = .25$ (i.e., $t/R = 10^{-2}$).

The value of thickness $t = 2.5$ (i.e. $t/R = 10^{-1}$) has not been dealt with since the case of thick shell does not give rise to locking phenomena. In Fig. 3 we present the numerical results relative to the case $t = 0.25$.

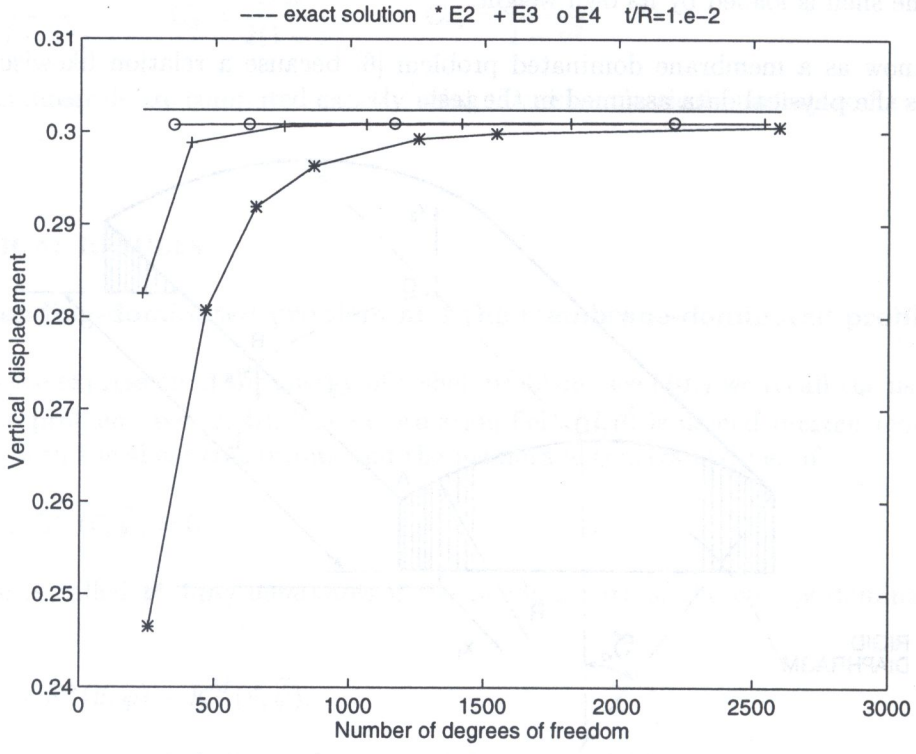

Fig. 3. Computed vertical displacement at the point B of Scordelis–Lo roof for $t = .25$ ft

We observe that the displacement at the midpoint B of the free edge has been computed and that the corresponding exact solution is 0.3024 ft (see [3]). More precisely, we show the behavior of the computed displacement at the point B, compared with the exact value, against the number of degrees of freedom, for the elements of degree $p = 2, 3, 4$. Let us denote, here and in the following, by E2, E3, E4, the finite elements of degree 2,3,4, respectively. We note that in this case we get satisfactory results with E2 and remarkable improvements are obtained with E3 and E4. This means that, in the range of values of practical interest, the finite elements are able to prevent the locking phenomenon. In Fig. 4 we show the results corresponding to the thickness $t = 0.025$ (i.e., $t/R = 10^{-3}$).

The thinning of the shell causes a small loss of convergence for E2, while using E3 and E4 no evidence of locking is exhibited. Finally, Fig. 5 shows the results obtained with $t = 0.0025$ (i.e., $t/R = 10^{-4}$), a very thin shell. As far as we know the exact solution is not available for this test. However, the results show good convergence properties for $p = 4$, while the results for lower values of p are unsatisfactory.

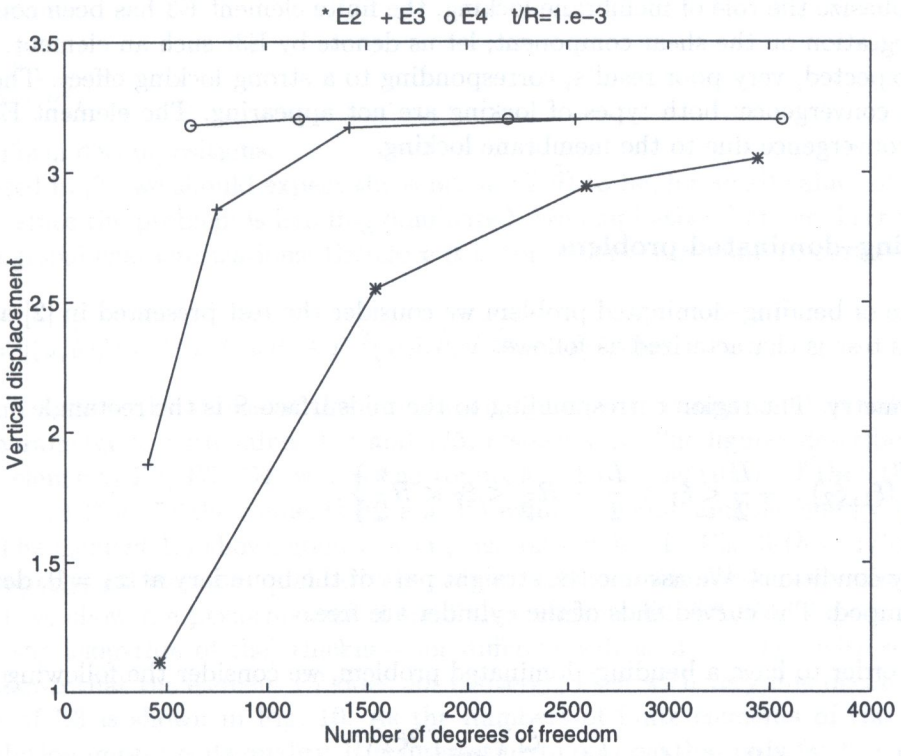

Fig. 4. Computed vertical displacement at the point B of Scordelis–Lo roof for $t = .025$ ft

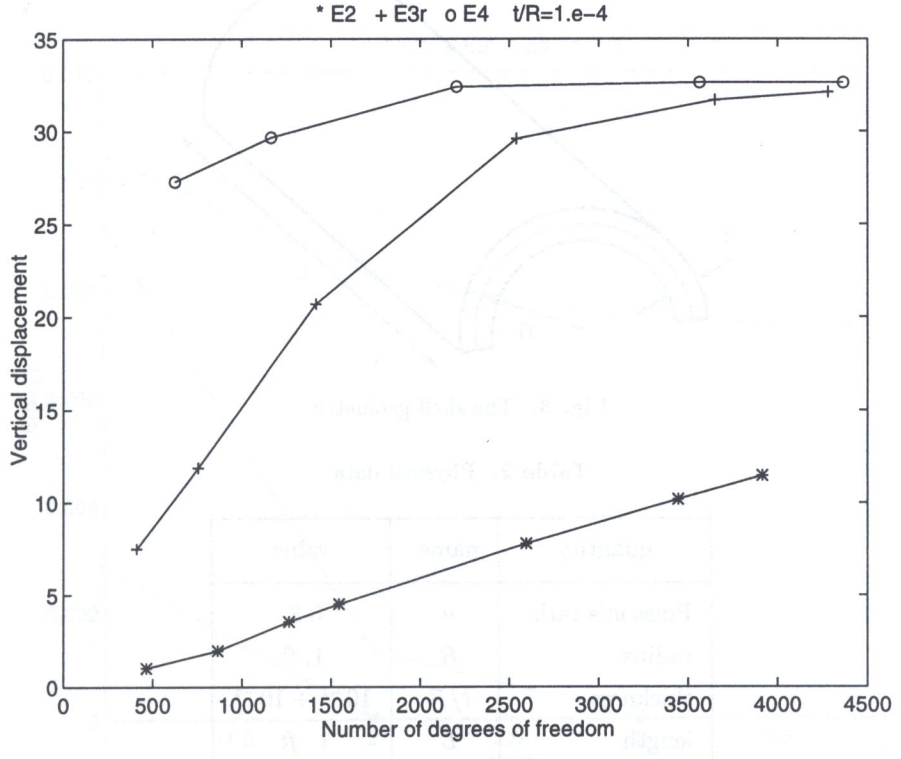

Fig. 5. Computed vertical displacement at the point B of Scordelis–Lo roof for $t = .0025$ ft

The test has been dealt with to analyse the behavior of both shear and membrane locking. Trying to emphasize the role of membrane locking, the finite element E3 has been computed using a reduced integration on the shear component; let us denote by E3r such an element. The element E2 gives, as expected, very poor results, corresponding to a strong locking effect. The element E4 shows a good convergence: both types of locking are not appearing. The element E3r exhibits a small loss of convergence due to the membrane locking.

3.3. A bending–dominated problem

As an example of bending–dominated problem we consider the test presented in [2] and described in Fig. 6. This test is characterized as follows.

(i) Shell geometry. The region corresponding to the midsurface S is the rectangle

$$\Omega = \left\{(\xi_1, \xi_2) : -\frac{L}{2} < \xi_1 < \frac{L}{2},\ -R\frac{\pi}{2} < \xi_2 < R\frac{\pi}{2}\right\}. \tag{28}$$

(ii) Boundary conditions. We assume the straight part of the boundary at $x_3 = 0$, denoted by Γ_0, to be clamped. The curved ends of the cylinder are free.

(iii) Load. In order to have a bending–dominated problem, we consider the following type of load

$$f_1 = 0, \qquad f_2 = 0, \qquad f_3 = \left(1 + \frac{\xi_1}{L}\right)\cos\left(\frac{2\xi_2}{R}\right). \tag{29}$$

Table 2 shows the physical data assumed in the test.

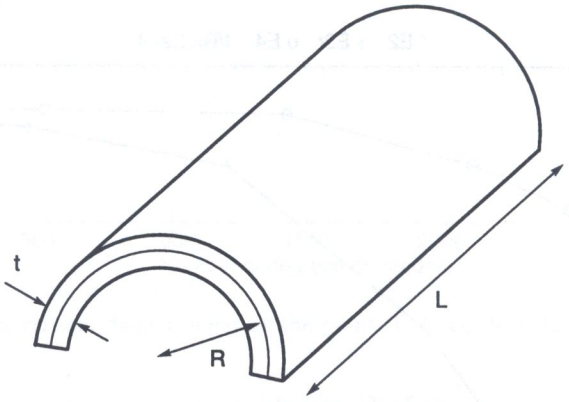

Fig. 6. The shell geometry

Table 2. Physical data

quantity	name	value
Poisson's ratio	ν	0.3
radius	R	1. ft
thickness	t/R	$10^{-1} \div 10^{-4}$
length	L	1. *ft*
angle	θ_0	$\frac{\pi}{2}$ rad

For sake of simplicity computations have been carried out after normalizing with respect to the material constant

$$K = \frac{E}{12(1-\nu^2)}$$

and with uniform decompositions.

As discussed in [2], we should expect the solution $(\vec{u}, \widetilde{\theta})$ to be, for small values of t, nearly independent of t, since the problem is bending dominated. We emphasize that the discriminations (24) and (25) are global characterizations; therefore it is convenient to compute the scaled deformation energy

$$E(\vec{u}, \widetilde{\theta}) = \|(\vec{u}, \widetilde{\theta})\|^2 = b(\vec{u}, \widetilde{\theta}; \vec{u}, \widetilde{\theta}) + t^{-2}(s(\vec{u}, \widetilde{\theta}; \vec{u}, \widetilde{\theta}) + m(\vec{u}, \vec{u}))$$

Figures 7 and 8 show the values of the discrete energy corresponding to fixed values of the discretization parameter h, with values $1/4$ and $1/5$, respectively. The figures describe the behaviors of the finite elements E2, E3, E4, versus the (opposite of the logarithm of the) thickness of the shell. For $h = 1/4$ (Fig. 7) the elements E2 and E3 exhibit locking and the energy approaches the zero value. The element E4 shows good convergence properties. In Fig. 8 ($h = 1/5$) only E2 does not work properly; E3 shows a qualitatively correct behavior while E4 give satisfactory results. In Figs. 9–11 we show the performances of the finite elements E2, E3, E4, respectively versus the (opposite of the logarithm of the) thickness for different values of $h = 1/n$ with $n = 2, \ldots, 8$. In Fig. 9 it is shown that the element E2 does not converge, even with very fine decompositions. The performance of E3 is shown in Fig. 10. As the numbers of finite elements of the decomposition grows the solution improves its quality. It is interesting to observe that only for $h > 1/5$ the locking effect is appearing. The behavior of E4, shown in Fig. 11, is quite good for $h \leq 1/4$, reasonable for $h = 1/3$ and poor for $h = 1/2$. Such conclusions agree with the remarks made in [2] where the Koiter–Sanders–Novozhilov model is applied. We note that this model differs from the one used here for the curvature component Υ_{22} in which the extra term $(1/R)[u_{2,2} + (1/R)u_3]$ appears.

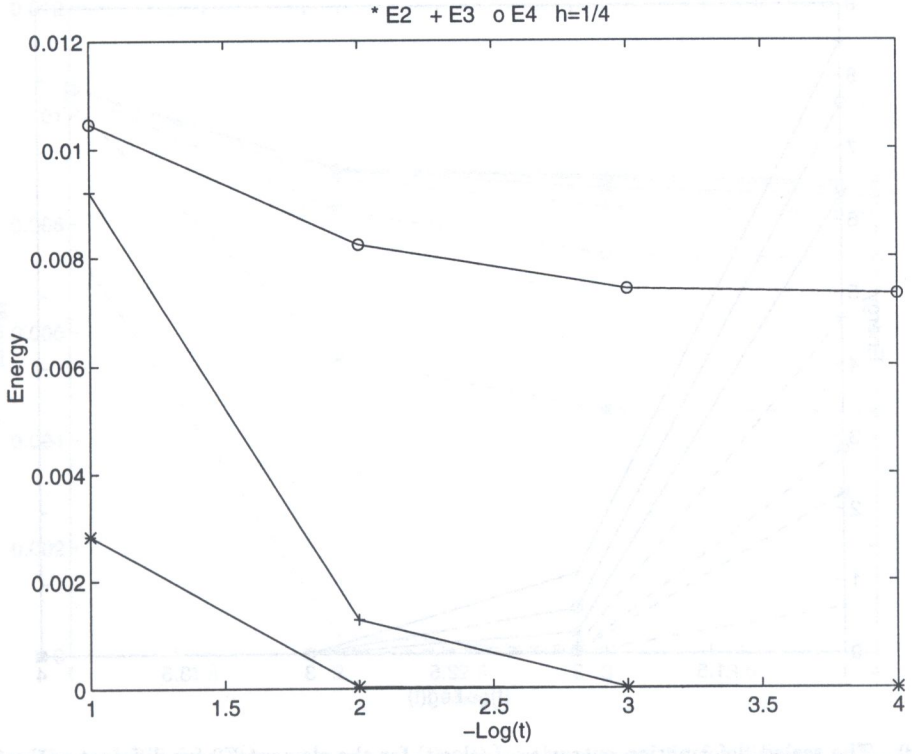

Fig. 7. The scaled deformation energy *vs.* $(-\log t)$ for E2, E3, E4 elements, $h = 1/4$

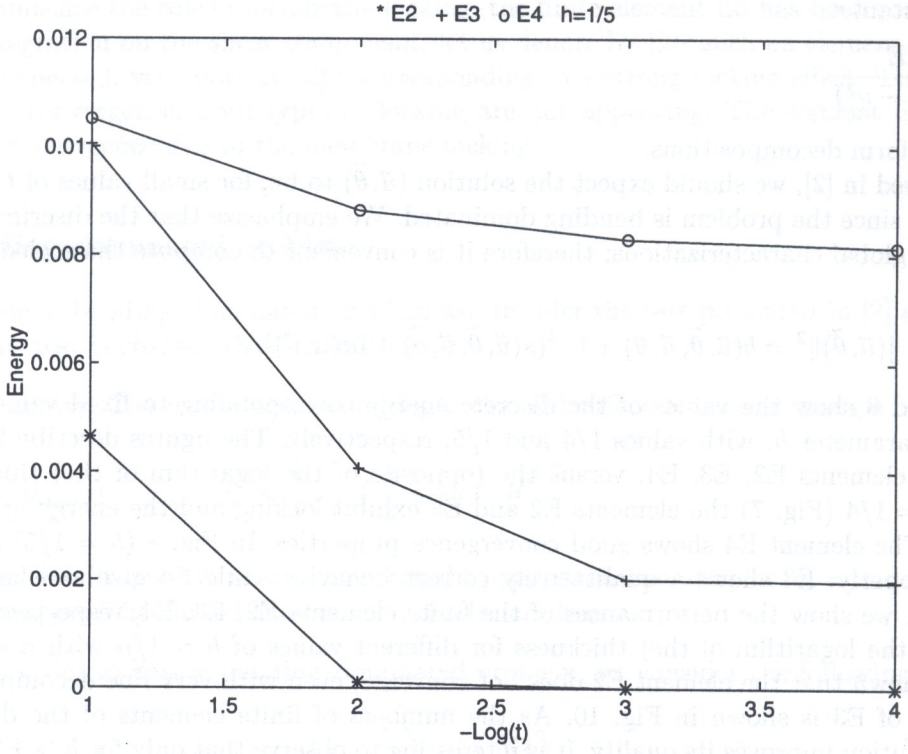

Fig. 8. The scaled deformation energy *vs.* $(-\log t)$ for E2, E3, E4 elements, $h = 1/5$

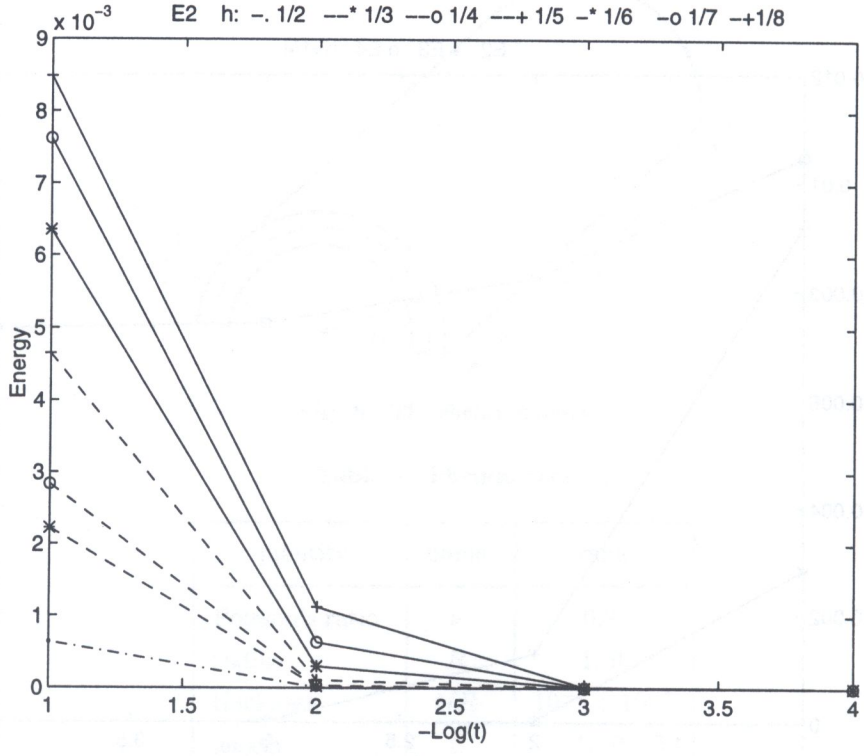

Fig. 9. The scaled deformation energy *vs.* $(-\log t)$ for the element E2 for different values of h

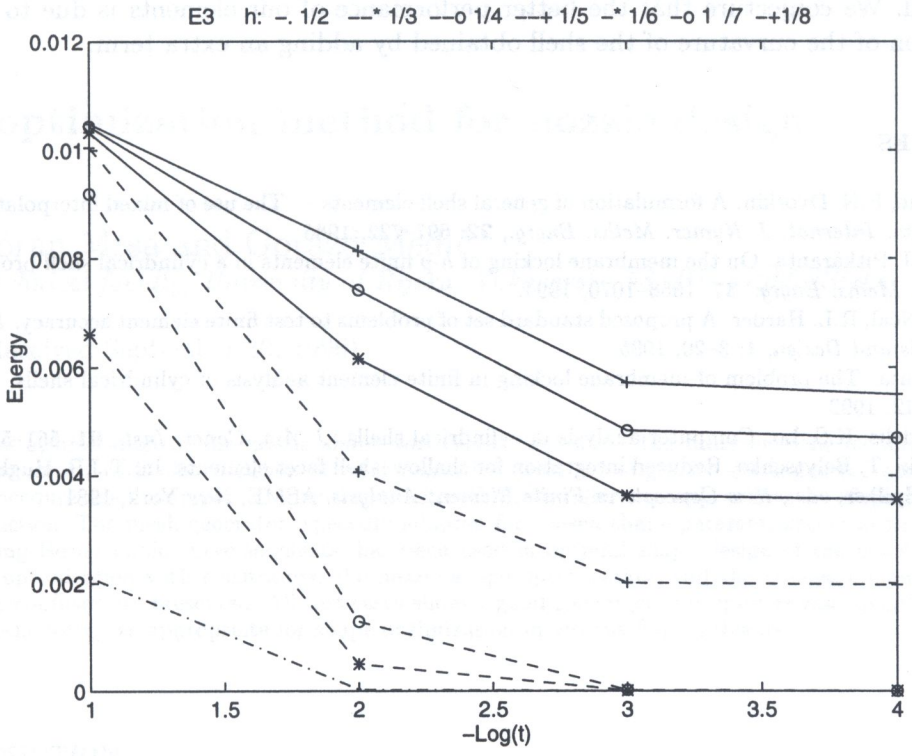

Fig. 10. The scaled deformation energy *vs.* $(-\log t)$ for the element E3 for different values of h

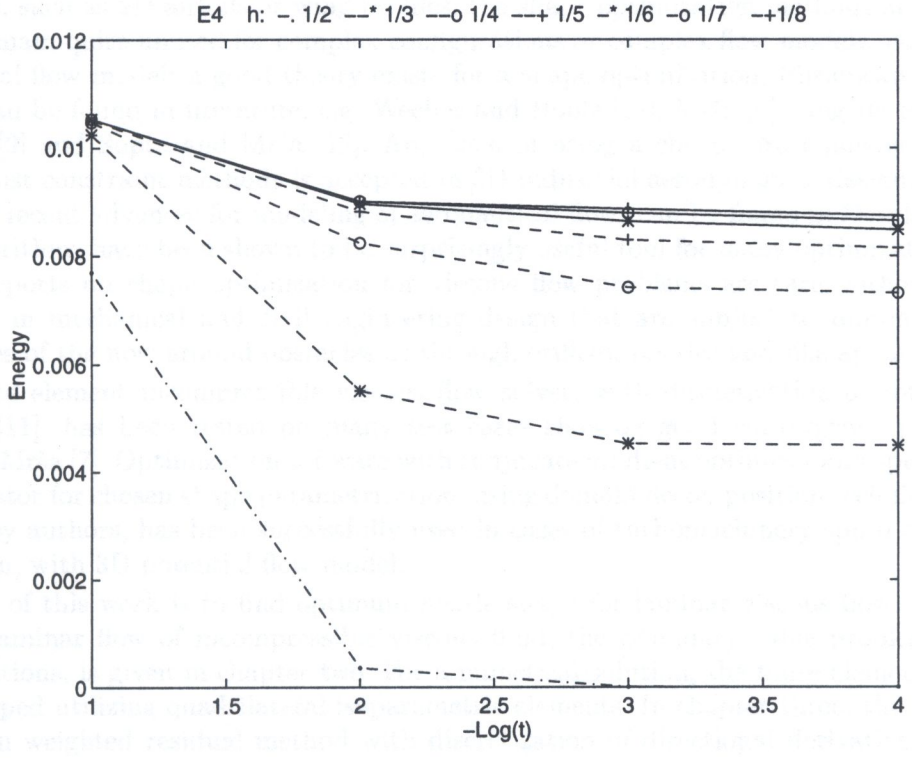

Fig. 11. The scaled deformation energy *vs.* $(-\log t)$ for the element E4 for different values of h

A comparison with the results presented in [2] shows an improvement with the finite elements we have used. We conjecture that the better performance of our elements is due to the different approximation of the curvature of the shell obtained by adding an extra term.

REFERENCES

[1] K.-J. Bathe, E.N. Dvorkin. A formulation of general shell elements — The use of mixed interpolation of tensorial components. *Internat. J. Numer. Meths. Engrg.*, **22**: 697–722, 1986.

[2] Y. Leino, J. Pitkäranta. On the membrane locking of *h-p* finite elements in a cylindrical shell problem. *Internat. J. Numer. Meths. Engrg.*, **37**: 1053–1070, 1994.

[3] R.H. MacNeal, R.L. Harder. A proposed standard set of problems to test finite element accuracy. *Finite Elements in Analysis and Design*, **1**: 3–20, 1985.

[4] J. Pitkäranta. The problem of membrane locking in finite element analysis of cylindrical shells, *Numer. Math.*, **61**: 523–542, 1992

[5] A.C. Scordelis, K.S. Lo. Computer analysis in cylindrical shells. *J. Am. Concr. Inst.*, **61**: 561–593, 1964.

[6] H. Stolarski, T. Belytschko. Reduced integration for shallow–shell facet elements. In: T.J.R. Hughes, D. Gartling and R.L. Spilker, eds., *New Concepts in Finite Element Analysis.* ASME, New York, 1981.